Computer Simulation and Percolation Theory Applied to Concrete

by

Edward J. Garboczi and Dale P. Bentz
Building and Fire Research Laboratory
National Institute of Standards and Technology
Gaithersburg, MD 20899 USA

Reprinted from Annual Reviews of Computational Physics, VII, Edited by Dietrich Stauffer, World Scientific Publishing Company, pp 85-123, 1999.

NIST
National Institute of Standards and Technology
Technology Administration, U.S. Department of Commerce

Annual Reviews of Computational Physics VII (pp. 85–123)
Edited by Dietrich Stauffer

COMPUTER SIMULATION AND PERCOLATION THEORY APPLIED TO CONCRETE

E. J. GARBOCZI and D. P. BENTZ
National Institute of Standards and Technology
226/B350, Building Materials Division
Gaithersburg, Maryland 20899 USA

Concrete is a multilength scale composite material. From the nanometer to the millimeter scale, it is a random composite, and a different random composite at each length scale. Percolation processes play a key role in the microstucture of concrete, and help to describe the overall dependence of transport properties like ionic diffusivity on the microstructure. Computer models have been developed to describe the microstructure and transport properties, as the randomness of the material precludes most (but not all) analytical formulations. The overall description of concrete, over six orders of magnitude of length scales, in terms of computer models, percolation theory, and composite ideas should be of interest to those studying other random materials as well, like ceramics and rocks. This report is written to present the ideas for concrete in such a way so as to be accessible to the noncement researcher. It is hoped that these ideas will prove to be useful in other materials.

1. Introduction

1.1. *The history and importance of concrete*

The Romans first invented what we call today hydraulic cement-based concrete. They built numerous concrete structures, including the Pantheon in Rome, one of the finest examples of Roman architecture that survives to this day, which has a 42-meter-diameter dome made of poured concrete.[1] The name concrete comes from the Latin "concretus," which means to grow together. This is a good name for this material, as the chemical hydration process, which mainly occurs over the time scale of hours and days, causes the material to grow together from a viscoelastic, moldable liquid into a hard, rigid solid. In our world today, concrete has become ubiquitous, and in fact it is hard to imagine modern life without it. More than five million million kilograms of

concrete are used around the world each year, enough for about one thousand kilograms for each person per year, at a volume of about 400 liters per person. The cement used mostly in today's concrete is called portland cement. The process to produce portland cement was invented by Joseph Aspdin in the early 1800's in England. The name portland may have been originally a marketing ploy, as portland building stone was very popular in England at that time,[1] and Aspdin may have wanted people to favorably compare concrete made with his cement to the popular building stone.

It is important to remember that cement is the powder that reacts with water to form cement paste — a hard, solid material that forms the matrix for the concrete composite. The addition of sand (fine aggregates) that are up to a few millimeters in diameter makes mortar, and the addition of rocks (coarse aggregates) of up to a few centimeters in diameter makes concrete. It has always been known that concrete is a porous material, whose properties depend on its pore space. There are many different kinds of pores in concrete, ranging from the air voids that are entrapped in the mixing process, which can be quite large, up to a few millimeters in diameter, to the capillary pores, which are essentially the space occupied by the leftover water from mixing, down to the nanometer-scale pores that exist in some of the hydration products produced by the cement–water chemical reaction.

Until recent years, the overwhelming focus has been on concrete's compressive strength, which has been mainly related to the overall porosity of the cement paste matrix and the amount and structure of the aggregates. Mechanical strength depends on defects and not on any overall average property, and so is very difficult to relate to microstructure. This has caused relatively little attention to be paid to the details of the pore space. Unfortunately, it has perhaps led to the the idea that concrete is simply a commodity material, with nothing needed to be understood about the microstructure. However, more recently, it has been recognized that much of the concrete in the infrastructure in the U.S. and Europe and elsewhere has been deteriorating faster than expected, with much of this deterioration due to the corrosion of reinforcing steel coming from the ingress of chloride and other ions from road salts, marine environments, and ground soils. Hence, close attention is now being paid to the transport properties of concrete (diffusivity, permeability, sorptivity, etc.) which, although are still difficult to relate to pore structure and microstructure, are easier to study in a fundamental way than compressive strength.[2] This has led to new attention being paid to the microstructure of concrete, with the

realization that concrete is a complex composite, whose improvement and control require the usual materials science approach of processing, microstructure, and properties.

This chapter briefly reviews some of the main ideas that have been proposed and partially validated to attempt to explain the microstructure of concrete and its effect on transport properties. The main ideas used are percolation and composite theory, combined with quantitative computer simulations. This chapter reflects the authors' view of concrete microstructure, and draws heavily on computer simulations of the microstructure. Not every part of this view has been validated experimentally, though much has, so that we expect some parts to change over time as new experiments (and new simulations!) are performed.

1.2. *The complexity of concrete microstructure*

Concrete is a composite material whose microstructure contains random features over a wide range of length scales, from nanometers to millimeters, with each length scale presenting a new random composite with which to deal.[3] In its actual uses, at the length scale of meters, concrete (almost always reinforced by steel) is usually considered to be a uniform material, with bulk properties like compressive strength, creep, and others. This is the usual engineering length scale.

Figure 1 shows three microscopic views of concrete, displaying the length scales of the material itself. In the left side of the figure, there is an optical micrograph of concrete. At this length scale, the concrete can be considered

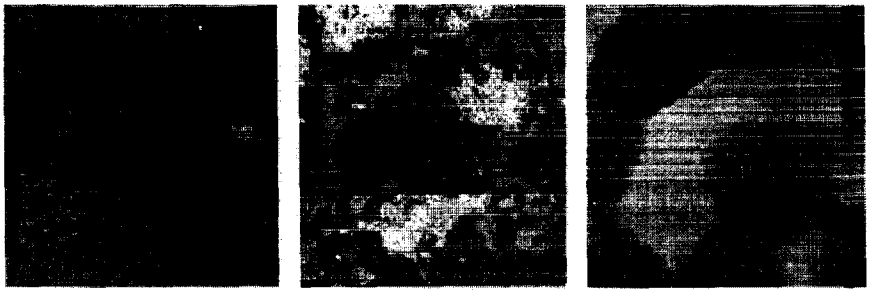

Fig. 1. Showing concrete at three different length scales: left [concrete (30×30 mm)], middle [cement paste (300×300 μm)], right [C–S–H (300×300 nm)].

to be a random composite, where the aggregates range from 0.25–30 mm, and the matrix is cement paste. The middle image shows a backscattered electron scanning electron micrograph of the cement paste matrix. The large white clumps are the largest of the unreacted cement grains, with the largest grains in the image being about 50–80 μm. The contrast in a backscattered electron scanning electron micrograph is provided by average atomic number, and so the unreacted cement grains are now the brightest phase. Cement paste is clearly a random composite material, made up of unreacted cement, capillary pores, and various other chemical phases that are a result of the hydration reactions between water and cement.[4] The main reaction product phase is an amorphous, or at best, poorly crystalline calcium silicate hydrate gel, produced via a hydration reaction and denoted C–S–H (in cement chemistry notation, C = CaO, H = H_2O, S = SiO_2, F = Fe_2O_3, A = Al_2O_3, $\bar{S}$ = SO_3). This is really the glue that holds the cement paste together, just as cement paste is the glue that holds mortar and concrete together. In the image, this is the gray that lines the cement grains and is clumped in-between, showing where small cement grains used to be before being consumed by the hydration reaction. The randomness in the cement paste microstructure is on the order of micrometers, because the original cement grains have an average diameter of approximately 10–20 μm, and these set the scale for the microstructure.

Finally, the right side of Fig. 1 is a transmission electron micrograph of C–S–H,[5,6] which is itself seen to be a complex material with a random porous nanostructure. The size of the image is about 300 nm on a side. This random nanostructure can also be detected by neutron scattering.[7]

The range of the random microstructure of concrete, from nanometers (C–S–H) to micrometers (cement paste) to millimeters (mortar and concrete) to meters (final end use) covers nine orders of magnitude in size! It is a large and difficult task to try to theoretically relate the microstructure and the properties of concrete. This has led to the use of computer simulations, coupled with modern experimental probes, which have provided some insight into the microstructure–property relationships of concrete.

2. Basic Concepts

Typical kinds of transport processes important in concrete are: (1) the transport of water, either due to a hydrostatic pressure head or wetting forces (capillary suction) and (2) the migration of ions, either due to diffusion under a concentration gradient, or to transport by moving water. For both of these

processes, how (and if) the relevant pores are connected to each other matters very much. Phrased more rigorously, the percolation properties of the random microstructure and particularly of the pore space are the critical geometrical and topological factors upon which the microstructure–transport property relationships are based.

The ideas of percolation theory are helpful in understanding the important features of random structures (see Ref. 8 for a review). The main concept of percolation theory is the idea of connectivity. Picture some sort of structure being built up inside a box by the random attachment of small pieces to each other. Percolation theory attempts to answer the question: at what point does the structure span the box? An alternate form of this question, for a random structure that already spans the box is: if pieces of the structure are removed at random, when will it fall apart? The percolation threshold is defined by the value of some parameter, say volume fraction of the structure in the box, right at the point where the structure either achieves or loses continuity across the box.

An example of percolation phenomena is displayed by the model of randomly placing freely overlapping objects in a matrix (this actually roughly simulates the growth of solids due to reactions like those seen in concrete). The objects gradually form larger and larger clusters, because they can connect via overlap, until a percolated structure is formed. This model has been studied extensively in 2-D and 3-D (see Refs. 9 and 10, and many references therein). Consider the following simple 3-D example. The objects used are overlapping spheres, placed at random positions in a 3-D matrix. The volume fraction covered by the collection of spheres is monitored until they form a continuous structure. It is found numerically that they will become continuous when they occupy approximately 29% of the total volume.[10] This is an example of the percolation of a structure that is being randomly built up. If the spherical objects become ellipsoids, then this critical volume fraction decreases as the ellipsoid aspect ratio either increases or decreases away from unity.[10] For the sphere case again, if we now think of the matrix as a uniform conducting material, and the overlapping spheres as insulators, then the composite material will lose its ability to carry an electrical current when the matrix loses connectivity at a matrix volume fraction of about 3%.[11] This is an example of the percolation of a structure that is being randomly torn down. Concrete exhibits both kinds of percolation processes, at more than one length scale.

3. Cement Paste

We now specifically consider the microstructure–transport property relationships in cement-based materials. We begin with cement paste, as this is the matrix material for the concrete composite, and it is difficult to understand the behavior of a composite without first understanding the matrix phase. Later we will consider mortar and concrete, composites made from cement paste at higher length scales, and individual phases of cement paste like C–S–H, at lower length scales.

The starting point for cement paste = cement + water, cement powder, is obtained by grinding cement clinker. The cement clinker is manufactured by firing mixtures of limestone and clay, which contain aluminate and ferrite impurities. After extraction from the kiln, gypsum (calcium sulphate dihydrate) is added to moderate the hydration process. After grinding together the clinker and gypsum, the cement powder consists of multisize, multiphase, irregularly shaped particles generally ranging in size from less than 1 μm to about 100 μm, with an average diameter of about 15–20 μm (color images of these particles are available at http://ciks.cbt.nist.gov/garboczi/, Chapter 4).

When the cement is mixed with water, all the chemical phases of the cement undergo hydration reactions that ultimately convert the water–cement suspension into a rigid porous material, which serves as the matrix phase for mortar and concrete. The nominal point of hydration at which this conversion to a solid framework occurs is called the set point. The degree of hydration at any time is the volume fraction of the cement that has reacted with water, and is often denoted by the symbol α. The ratio of water to cement in a given mixture is specified by the water to cement ratio (w/c), which is the ratio of the mass of water used to the mass of cement used. An ordinary concrete used in buildings uses cement paste with $w/c \approx 0.5$. Newer high performance concretes often have w/c ratios of 0.3 or lower.[13]

The various chemical and mineral phases within the cement powder hydrate at different rates, depending on their size and composition, and interact with one another to form various reaction products. Some products deposit on the remaining cement particle surfaces (surface products), while others form as crystals in the water-filled pore space between cement particles (pore products). For simplicity, and because it still correctly captures the main features of the pore structure, cement paste can be thought of as consisting of four phases: (1) unreacted cement, (2) surface products (like C–S–H), (3) pore products

(like CH = calcium hydroxide), and (4) capillary pore space. Surface products grow outward from the unreacted cement particles and contain connected (percolated) gel pores, while pore products are generally polycrystalline and fully dense, with no connected pores. The capillary pores are the remaining water-filled space between solid phases, left over after a given degree of hydration takes place. Capillary pores generally range from about 0.01–0.1 μm in size, in a reasonably well-hydrated cement paste ($\alpha > 0.5$), although in early hydration, they can range up to a few micrometers in size.

While images of both initial and hydrated cement microstructures can be experimentally obtained in two dimensions, acquiring quantitative three-dimensional information is much more difficult. It is for this reason that computer models of the 3-D microstructural development of cement paste have been developed.

The actual process of cement hydration, for the purposes of modeling the development of microstructure, can be broken down into three parts: (1) material dissolves from the original cement particle surfaces, (2) diffuses within the available pore space, and (3) ultimately reacts with water and other dissolved, or solid species to form hydration products. Therefore, in order to simulate the microstructure development of hydrating cement, the physical processes of dissolution, diffusion, and reaction must be simulated. Each of these processes may be conveniently simulated using cellular automaton-type rules as have been previously described.[14,15] Figure 2 shows four steps of simulated hydration for a C_3S cement paste in 2-D. C_3S is the main phase of portland cement. Its hydration characteristics are a useful and reasonable model of those of the entire cement. The original particle shapes are taken from a backscattered SEM image. The gray levels of the images show the major phases of portland cement.[14]

This brief description of the chemical hydration process, which is the basis of the microstructural formation of cement paste, of course, glosses over a number of chemical details, many of which are not clearly understood.[14] However, this simple description is sufficient to be able to go on and investigate the various important percolation thresholds that occur in cement paste.

3.1. *Solids percolation: Set point*

Immediately after mixing cement powder and water together, the solid phases are discontinuous, or connected only via van der Waals-type forces,[16] and so the freshly mixed cement paste is a viscous liquid. The solid phase is then built

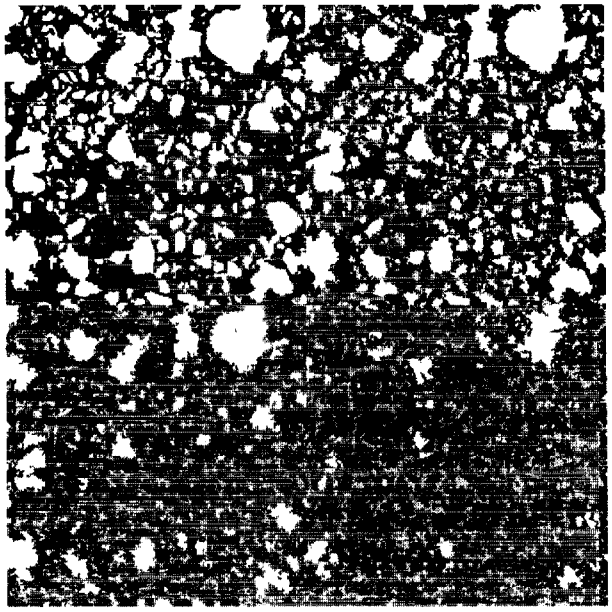

Fig. 2. Showing four stages of hydration in a microstructural model of C_3S hydration. The degrees of hydration are: top left–0, top right–20%, bottom left–50%, bottom right–87%. White = unreacted cement, light gray = CH, dark gray = C–S–H, and black = porosity.

up through random growth of reaction products, and at some point becomes continuous across the sample, mainly due to the formation of the C–S–H surface products.[17] Experimentally, this setting process can be detected using a needle penetration test,[18] ultrasonic shear wave propagation,[19] or by measuring the shear strength of the paste.[16,20] The set point can be defined rigorously, using percolation concepts, as the point where percolation of the total solid phase occurs. This point can be computed, using a three-dimensional computer model based on a simplified cement composed only of monophase C_3S particles. This chemical simplification of the particles is justified by the experimental observation that the C–S–H surface product causes set[17] and by the fact that this simple model generates almost the same quantity of surface products as those produced in real cements.[21] Also, most real portland cements are usually composed of at least 60% C_3S.

Using this model, in conjunction with a burning algorithm[21] to compute connectivity, one can determine the degree of hydration necessary to first have

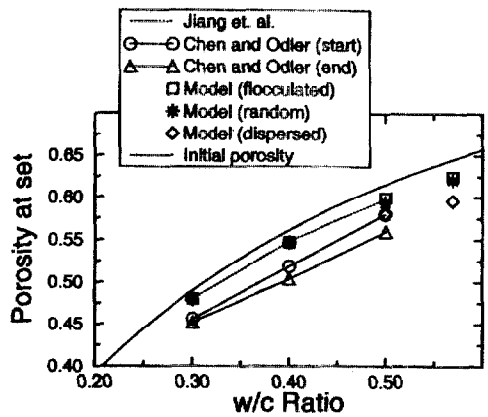

Fig. 3. Showing the capillary porosity remaining at the set point, for several experimental and model cement pastes involving different initial cement particle configurations, as a function of the w/c ratio of the cement paste.

a continuous network of cement particles linked by C–S–H gel product. This seems to be a reasonable definition of set, especially since the combined phase of cement and C–S–H will percolate before any individual solid phase. In addition, the original configuration of the cement particles can be simulated as being flocculated or dispersed. Figure 3 shows a quantitative comparison between model and experimental results.

The data from Jiang *et al.*[20] were calculated as the capillary porosity at the point where the cement paste exhibited a shear resistance of 0.08 MPa. The data points of Chen and Odler[17] correspond to the measured porosities at the beginning and end of set according to the ASTM standard needle penetration method.[18] Model results, corresponding to the point when a spanning cluster of C_3S particles connected together by the C–S–H gel first exists, are presented for flocculated, random, and dispersed systems based on a discretized version of a real-measured particle size distribution.[22,23] In general, the comparison among these three data sets is reasonably good, particularly so for the experimental data of Jiang *et al.*[20] and the model results of the random/flocculated systems. As the w/c ratio decreases, less hydration is needed to achieve set, since the initial interparticle spacing is less. Based on the model results of the random systems, degrees of hydration of 1.8%, 2.7%, and 4.6% are required to achieve solids percolation for w/c ratios of 0.3, 0.4, and 0.5. The capillary porosities at set obtained by Jiang *et al.*[20] are consistently higher than those of

Chen and Odler,[17] suggesting that the ASTM needle penetration test method measures set time based on a resistance somewhat greater than that corresponding to a shear strength of 0.08 MPa. As might be expected, in general, the model flocculated systems require less hydration to achieve set than their dispersed counterparts, in agreement with experimental studies.[24,25] It should be noted that the experimental measurements were generally made on portland cements while the model results are for C_3S pastes. However, the similarity in volumes of surface and pore products formed for these two pastes[21] allows valid comparisons to be made between model and experimental results.

Because it is the connection of cement grains by C–S–H gel product that regulates set, a finer particle size cement will actually require a greater degree of hydration to achieve set than a coarser one. Thus, even though a finer cement typically hydrates at a faster rate, it may lead to a longer setting time than a coarser, slower hydrating cement, where fewer particle-to-particle contacts are necessary to achieve set, as has been verified experimentally.[16] This analysis assumes that the volume of C–S–H product needed to connect two cement particles is roughly invariant, so that as the particle size increases at a fixed total volume of cement, the number of particles, and therefore, the number of connections needed will decrease.[26]

3.2. *Capillary pore space percolation*

A percolation threshold that is more important for transport processes is the point at which the capillary pore space no longer percolates. Such a percolation threshold can exist, because as hydration products are formed, pieces of the capillary pore space will be trapped and cut off from the main pore network, thus reducing the fraction of the pores that form a connected pathway for transport. As this process continues, the capillary pore space can lose all long-range connectivity, so that fast transport of water or ions through the relatively large capillary pore system would end, and slow transport would then be regulated by the smaller C–S–H gel pores (pore product).

Computer simulation of cement hydration in 3-D is a means of computing such a percolation threshold. Figure 4 shows the fraction connected of the capillary pore space versus degree of hydration for several w/c ratios, as computed by a computer simulation model of cement paste microstructure.[21] The quantity fraction connected is defined as the volume fraction of capillary pores that make up a connected path through the sample, divided by the total volume fraction of capillary pores.

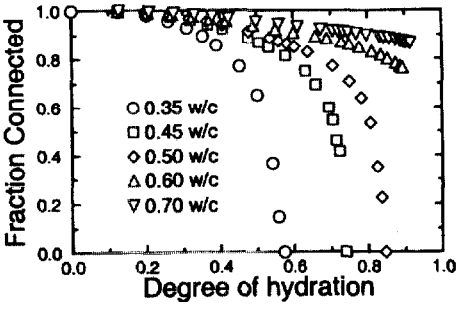

Fig. 4. Showing the fraction of the capillary pore space that is part of a percolated (continuous) cluster, for several different w/c cement pastes as a function of degree of hydration.

Immediately after mixing, the cement particles are totally isolated, assuming adequate dispersion, and so the connected fraction of the capillary pore space is one. As hydration occurs, the connected fraction decreases gradually. If continuity is lost at some critical degree of hydration, the fraction connected will go to zero. Such a percolation threshold can be seen in all of the w/c ratio results plotted, except for 0.6 and 0.7. We have found in the model that w/c ratios of 0.6 and above always have a continuous (or percolated) capillary pore system. This prediction is in good agreement with experiment.[27] It is clearly seen in Fig. 4 that as the w/c ratio decreases below 0.6, less and less hydration is required to close off the capillary pore system.

In order to unify the previous results, we have replotted all the data from Fig. 4 in Fig. 5 against capillary porosity. All the connectivity data now falls on

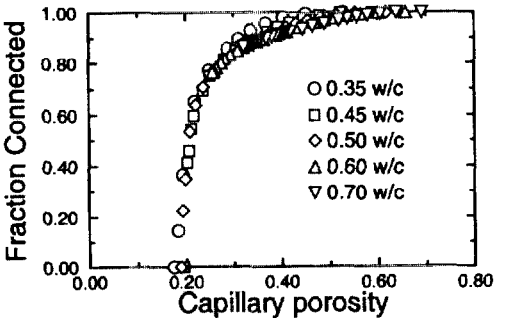

Fig. 5. Showing the fraction of the capillary pore space that is part of a percolated (continuous) cluster, for several different w/c cement pastes as a function of capillary porosity.

one curve, and it is clearly seen that there is a common percolation threshold at a critical value of capillary porosity of about 0.18.

Even the 0.6 and 0.7 w/c data fall on this curve, and now it is clear why these pastes always have an open capillary pore space: there is not enough cement present originally to be able to bring the capillary porosity down to the critical value, even after full hydration. The capillary pore space percolation threshold for cement paste will have some sensitivity to cement particle size distribution and degree of dispersion, so that the critical value of capillary porosity for percolation should be considered to be about $18 \pm 5\%$. This range of values is a rough estimate of finite system size and particle size distribution effects, based on computation on different systems.

The percolation threshold is also sensitive to the morphology of the reaction products, reminscent of the simple overlapping object percolation problem.[10] For example, in a simple dissolution/reaction model, in which only a pore product is formed, capillary porosity percolation thresholds have been computed to be in the order of 20% for totally random morphology products, 25% for 1-D needle-like products, and 30% for plate-like products.[28]

3.3. *C–S–H percolation*

As was discussed above, the percolation of the combined cement — C–S–H phase determines the set point, or the rigidity threshold. The model described above also, however, predicts a percolation threshold for the C–S–H phase by itself. The prediction is that the C–S–H phase, independent of w/c, will percolate when its volume fraction is about 20%.[21] This will be fairly early in the hydration process, but well after the set point. Since this percolation threshold is not usually connected to a physical observable at this stage, it is difficult to experimentally validate this prediction. Recently, however, electrical measurements at low temperature ($-40°C$) have been able to confirm this prediction. Both the capillary pores and the C–S–H pores serve as conducting channels, since they are filled with the electrolytic pore solution.[29] At lower temperatures, the water in the larger capillary pores freezes while that in the smaller C–S–H pores does not. In this case, the electrical conductivity of the capillary pores is turned off, and the only conductivity comes from the C–S–H pores. If the C–S–H phase is not percolated, then the conductivity should be very small. Figure 6 shows the conductivity at a temperature of $-40°C$, normalized by the pure C–S–H conductivity and plotted versus volume fraction of C–S–H. There is a clear percolation threshold at around 20% volume fraction,

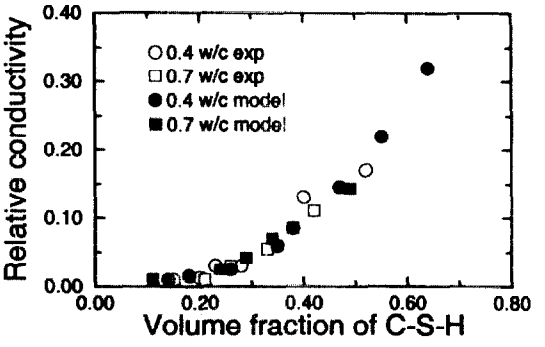

Fig. 6. Showing the electrical conductivity of the cement paste at −40°C, plotted versus the volume fraction of C–S–H. The solid symbols are model results, and the open symbols represent experimental values.

validating the predictions of the model.[30] There is also excellent agreement between model and experimental values for all the volume fractions of C–S–H examined. The simple fact that the conductivity goes *up* with hydration shows that at this temperature, the conductivity is coupled to the growing C–S–H phase, not the shrinking capillary porosity phase.

3.4. *Cement paste pore size*

During hydration, the capillary pore size, as well as the overall capillary porosity, decreases due to consumption of water during hydration, producing hydration products that fill in the capillary pore space. The size of the gel pores are fixed by the nanostructure of the C–S–H, however, and so remain relatively constant in size. As hydration continues, the size of the smallest capillary pores decreases to roughly the 10 nm gel pore size.[2,31] Therefore, the importance of the pure capillary pore transport paths decreases with time due to decreasing capillary pore size as well as decreasing pore connectivity.

3.5. *Diffusivity of Cement Paste*

Building on the percolation and pore size results given above, the dependence of the diffusivity of cement paste on pore structure can now be qualitatively outlined. Early in the hydration process the capillary pore space is fully percolated. These pores are much larger than the C–S–H gel pores (which are themselves also fully connected fairly early in the hydration process[21]) and so dominate the transport. As the capillary porosity decreases, the capillary pores

become smaller and only partially connected, so for porosities near but above the percolation threshold, pure capillary pore paths have only slightly more influence on flow than the hybrid paths that are made up of isolated capillary pockets linked by C–S–H gel pores. The capillary pores are still somewhat bigger than the gel pores, but their connectivity is decreasing. Below the critical capillary porosity, all flow must now go through C–S–H gel pores, but flow will be dominated by paths that still contain some isolated capillary pore regions, and are not just made up of pure C–S–H gel pores. If this were not true, then after a certain point, the diffusivity would begin going up with increasing hydration, since more C–S–H, and thus more gel pores, were being formed. This has not been observed in cement paste.[32]

The same microstructure model used to predict the connectivity results shown in Figs. 4 and 5 can also be used to compute the diffusivity of cement paste by solving Laplace's equation in the pore space with a finite difference method.[32] Because of the Nernst–Einstein relation,[32,33] relating diffusivity and conductivity, the same mathematical apparatus can be used for both, so that solutions to the time-independent Laplace's equation apply equally well to diffusivity or conductivity. If D_o is the ionic diffusivity in free water, σ_o is the conductivity of the electrolytic pore solution, D is the measured diffusivity of the porous material, and σ is the measured conductivity of the porous material, then the physical content of the Nernst–Einstein relation is that $D/D_o = \sigma/\sigma_o$. This computational procedure can be done for the DC and also for the frequency-dependent AC conductivity.[34,35] Computational results confirm the above microstructural picture, and compare reasonably well to experimental measurements.[32,34–36]

Figure 7 shows comparisons between experiment and model results for a 0.5 w/c cement paste.[36] The quantity $\Gamma = \sigma/\sigma_o$ is called the relative conductivity or diffusivity.[32,36] The value of σ_o was found by first squeezing out the electrolytic pore solution in a high-pressure press, and then measuring the conductivity of the pore solution in an impedance spectrometer.[36] A reasonably good comparison exists between simulation and experiment over a wide range of capillary porosity, indicating that the capillary pore space of the model compares well to that of real cement paste. The model results are from an equation that was fit to the results shown in Fig. 8.[32] They were determined from fairly low porosities, and so are not expected to fit well at high porosities. The agreement across all porosities is within a factor of two, however. The $\phi^{1.5}$ power line shown is the result for suspensions of insulating,

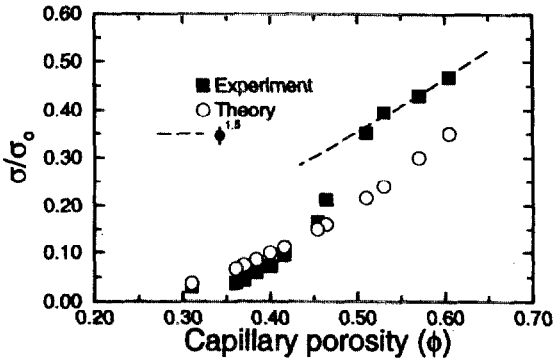

Fig. 7. Showing cement paste conductivity results, normalized by the pore fluid conductivity, for an 0.5 w/c cement paste as a function of the capillary porosity.

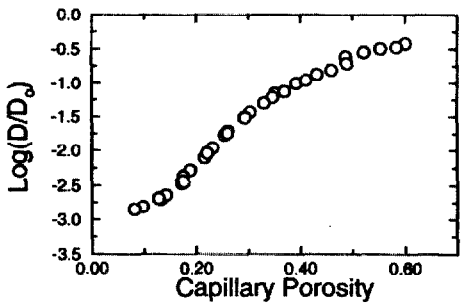

Fig. 8. Showing model data for the diffusivity for several different w/c cement pastes, normalized by the free water diffusivity, all plotted versus capillary porosity.

reasonably spherical objects suspended in a conducting medium. When hydration begins, ions are released into the mixing water, turning it conductive, while the cement simply acts as suspended insulating particles, which grow in size with hydration and so increase in volume fraction $1 - \phi$. However, as can be seen in the figure, the hydrating cement paste quickly changes its topology as the solid phase connects (set point), and the measured conductivities drop below the $\phi^{1.5}$ curve.

Figure 8 shows a collection of model results for Γ for different w/c values, all plotted against capillary porosity. Notice how all the data falls on a single master curve, as did the capillary pore space percolation data, when plotted against capillary porosity.[32]

Such a qualitative result has been observed experimentally as well,[37] lending support to the basic correctness of the model and the percolation picture of cement paste pore structure. A recent review (and references therein) may be referred to for more details of the electrical conductivity/ionic diffusivity of cement paste.[38]

3.6. *CH percolation: Leaching*

We can now combine the percolation and diffusivity simulations and ideas to study the problem of CH (pore product) leaching in cement paste. As concrete is exposed to the elements, its underlying microstructure can be attacked by a variety of aggressive agents. For example, rainwater and groundwater can degrade the concrete by dissolving soluble constituents such as calcium hydroxide. Using computer simulation, we can study the effects of calcium hydroxide dissolution on: (1) the percolation properties of the capillary pore space and (2) the relative ionic diffusivity.

The microstructure model shown in Fig. 2 for C_3S cement paste was used to produce a hydrated specimen which was subsequently subjected to the leaching process in which CH was randomly removed. This specimen can start with either a percolated or a disconnected capillary pore space. From a percolation perspective, the key point is the connectivity of the combined capillary porosity and calcium hydroxide phases. If these two phases together form a connected pathway across the microstructure, the capillary porosity will certainly be percolated when the calcium hydroxide is leached away, regardless of its initial percolation state. Based on computer simulation, a volume fraction of 16–20% for the combined capillary porosity and leachable calcium hydroxide phase is sufficient to form a percolated pathway after leaching has taken place.[39]

The computer models have also been applied to computing the increase in diffusion coefficients due to the leaching of calcium hydroxide from fully hydrated C_3S pastes of various w/c ratios.[39] The removal of all the CH from a cement paste can result in a multiplicative increase in diffusivity of up to about 50 times that of the original paste, as computed from the model, if the unleached paste had a disconnected capillary pore space, and leaching reconnected it. In Fig. 9, model values are compared with experimental results[40] in which the diffusion coefficients of cesium and tritium were measured as a function of the amount of CH leached out of portland cement paste specimens. Reasonable agreement is exhibited between the model and the available experimental results.

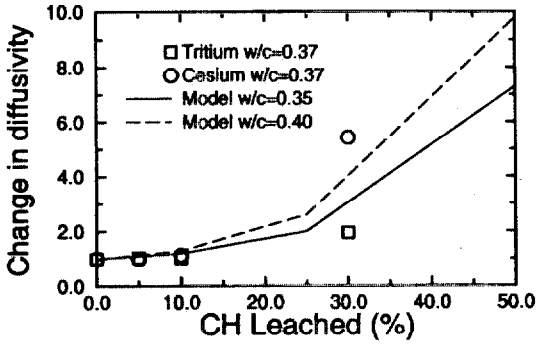

Fig. 9. Showing experimental and model results of how the relative diffusivity changes as the amount of CH leached away increases.

4. Microstructure of Mortar and Concrete

Mortar and concrete are random composite materials, with the fine and coarse aggregate acting as the inclusions, and the cement paste acting as the matrix. The only real difference between mortar and concrete is in the size of the aggregates used. Typically, the maximum aggregate diameter in a mortar is 1–3 mm, while the maximum aggregate diameter in a commercial concrete is around 30 mm. Concrete used for dams and other such structures, known as mass concrete, can have aggregate diameters even up to 150 mm or so.[41]

To handle mortar and concrete theoretically, we average out the cement paste micrometer length scale to avoid having to deal with microstructures on too wide a range of length scales at the same time. The transport properties of the aggregate are measurable and usually constant in time, while the transport properties of the cement paste depend on the original water: cement ratio, kind and quantity of admixtures, hydration time, and to some degree on the initial particle size distribution. However, it will be shown below that the interfacial transition zone between the cement paste and aggregates may play a critical role in determining the bulk transport properties.[42] Therefore, when averaging over the cement paste microstructure, the micrometer scale interfacial transition zone, which is determined from cement paste microstructure, must not be omitted. This makes the concrete random composite problem difficult, since micrometer and millimeter length scales have to be simultaneously considered. Also, mortar and concrete have aggregate volume fractions

of up to 70% or so, which implies that the spacing between particle surfaces is on the order of 100 μm, as seen by SEM in cross-section.[43] Therefore, the micrometer cement paste scale can also clearly come in here, especially, as we will see below, as the interfacial zone is itself in the order of 20–50 μm. There has also been some work using x-ray microtomography to directly image the aggregate–matrix structure in mortars, and in particular the spacing between aggregate surfaces, in 3-D.[44]

4.1. *Interfacial zone microstructure*

Characteristic features of the interfacial transition zone, that region of the cement paste close to an aggregate surface, have higher capillary porosity and larger pores than in the bulk cement paste matrix.[45,46] These features are typically seen in the cement paste that is within 50 μm of an aggregate surface.[47] Using the cement paste microstructure model mentioned above, we have analyzed two major causes of these features in the interfacial transition zone microstructure: (1) the particle packing effect and (2) the one-sided growth effect.[48]

The particle packing effect arises from particles not packing together as well near a flat surface as in free space. Since the typical aggregate is many times larger than the typical cement particle, even for the fine aggregate, locally the aggregate surface appears flat to the surrounding cement particles. This inefficient packing causes less cement and higher porosity to be present initially near the aggregate surface, and so even after hydration this condition persists. The width of the interfacial transition zone will then scale with the median cement particle size.[49] This is the main contribution to the interfacial transition zone microstructure, but not the only one.

The one-sided growth effect arises in the following way. Consider a small region of capillary pore space located out in the bulk paste part of a mortar or concrete. On the average, there is reactive growth coming into this small region from all directions, since the cement particles are originally located randomly and isotropically. Now consider a similar small region of capillary pore space, but located very near an aggregate surface. Reactive growth is coming into this region from the cement side, but not from the aggregate side.[48] This will give rise to a higher porosity, as the net growth of solids will then be smaller in the interfacial transition zone region.

4.2. *Concrete considered as a composite material*

If we were to make a concrete using cement paste and zero porosity aggregate, with no interfacial transition zones present, the ionic diffusivity and fluid permeability of the concrete would rigorously have to be lower than the corresponding values for the cement paste, as predicted by analytical bounds like the Hashin bounds.[51] This is because the aggregates, assumed to be fully dense, would have transport coefficients of zero, so that the mixture must have lower bulk properties, which can only decrease as more of the second phase (aggregate) is added. However, having a third phase, the interfacial transition zones can modify this picture.

The study of the transport properties of concrete using composite theory then requires, as experimental input, simultaneous measurement of the cement paste host and concrete transport properties, while the aggregate volume fraction is systematically varied. Unfortunately, there are not many experimental results available.[52,53] Results from recent work, however, demonstrate that the effective transport properties of concrete can increase greatly as more aggregate is added past a critical amount.[54] There are also data showing that concrete can have up to 100 times the water permeability of the cement paste from which it is made.[2] Experimental results for the ionic diffusivity show effects beyond that of simply adding insulating, nonporous aggregate to a porous phase.[52,53] Elastic modulus data also clearly show the effect of a third phase, the interfacial transition zone phase.[55–57] The only possible microstructural explanation of all this behavior, besides that of an unreasonable amount of microcracking, is the effect of transport of fluid or ions through the interfacial transition zones. It is already known that the interfacial transition zone regions contain pores larger than those in the bulk paste. However, if the interfacial transition zones do not percolate, their effect on transport will be fairly small, as any transport path through the concrete would have to go through the bulk cement paste. Transport properties would then be dominated by the bulk cement paste transport properties.

Before exploring the interfacial transition zone percolation problem further, it is important to note that real concrete always contains air voids, especially in air-entrained concrete, where air voids are introduced deliberately to help the porous material resist freeze–thaw damage.[58,59] The volume fraction of air voids can be as great as 5–10%, so they are an important constituent of concrete.[58,59] As long as they remain filled with air, they can be treated in a

transport model simply as more zero-property aggregate, with a known size distribution,[58,59] since the presence of air voids also causes interfacial transition zone regions to develop.[60]

4.3. *Interfacial zone percolation*

The fact that mercury is nonwetting for most porous materials at room temperature makes it convenient to use for measuring approximate pore size distributions via mercury injection experiments.[61–63] The pressure P required to force a nonwetting fluid into a circular cross-section capillary of diameter d is given by the Washburn equation:

$$P = 4\Gamma \cos(\theta)/d, \tag{1}$$

where Γ is the surface tension of the mercury and θ is the contact angle of the mercury on the material being intruded. By gradually increasing the pressure applied to a porous sample immersed in a mercury bath, and monitoring the incremental volume of mercury intruded for each increase in applied pressure, the pore size distribution of the sample can be estimated in terms of the volume of pores intruded at a given diameter d, by converting an intrusion pressure into a pore diameter via the Washburn equation.

Effects of the percolation of the interfacial transition zones can be observed from mercury porosimetry data.[64] Cement paste by itself has a threshold pore diameter, corresponding to a certain mercury pressure. For mercury pressures below this value, the mercury only intrudes the surface of the sample. For mercury pressures above this value, the mercury percolates throughout the material. When aggregate is added, this threshold diameter does not increase at first, but remains at a value typical of cement paste. As the volume of aggregate increases to a critical value, the mercury breakthrough pressure or critical diameter abruptly changes from values typical of bulk cement paste to those typical of the interfacial transition region, pore sizes roughly ten times bigger. This is interpreted as the point at which there are enough aggregates present so that the associated interfacial zones can overlap and percolate.[64]

To study the percolation or connectivity of the interfacial transition zones in concrete is computationally not simple, as the geometry of this phase is complex. Fortunately, in the percolation literature there is a model that is perfectly suited for this study, the hard core/soft shell (HC–SS) model.[65] This model starts with a random suspension of hard spherical particles, which are hard in the sense that they are packed without being allowed to overlap, as in

a suspension. Then concentric spherical shells are placed around each particle, where the spherical shells all have the same thickness, and are allowed to freely overlap. The volume fraction of shells required to make the shells percolate, which is when a continuous soft shell pathway first becomes established, is then computed. The volume fraction of soft shells required for percolation is a function of how many hard core particles are present, and the thickness of the soft shell. Obviously, when more hard core particles are packed in a given volume, there is less space between them, so that thinner soft shells will be sufficient for percolation. When there are fewer hard core particles present, thicker shells will be required for percolation of the shell phase. For concrete, clearly the hard cores correspond to the aggregates, and the soft shells to the interfacial transition zones. In the percolation literature, usually the value of h varies for different radii (r_i) particles, such that the ratio $(r_i + h)/r_i$ remains constant for different radii r_i. In the case of concrete, the value of h remains constant for different particle radii, which implies that this ratio is different for different radius particles.

Figure 10 shows a two-dimensional slice through a simple HC–SS three-dimensional model of a mortar, where four different sizes of spherical sand grains were used, ranging between 0.5 and 3 mm in diameter.[66] Note that there are more than four diameters of particles apparently present in the picture,

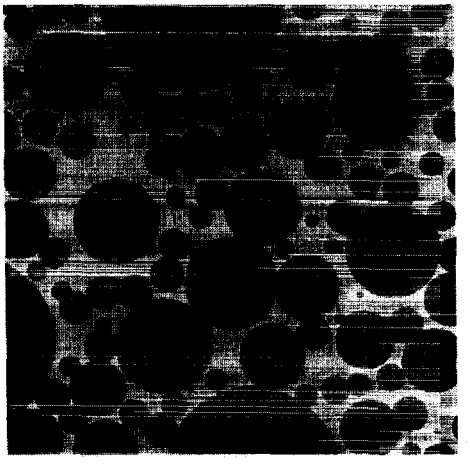

Fig. 10. Showing a slice of a three-dimensional model of mortar, with four aggregate diameters (dark gray) ranging between 0.5 and 3 mm, embedded in cement paste (light gray). The interfacial transition zone is shown as black.

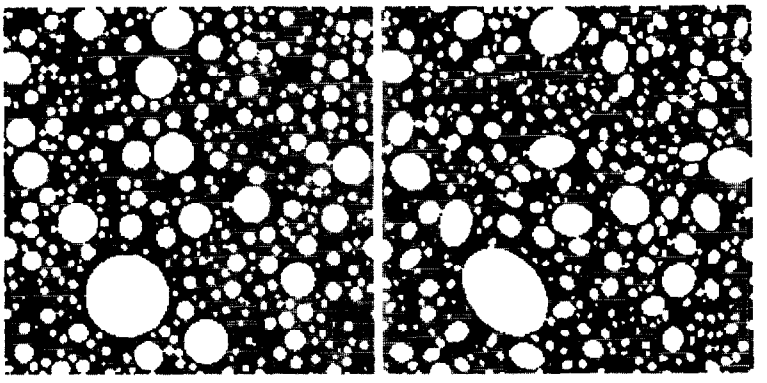

Fig. 11. Showing slices of two different three-dimensional concrete models, with spherical- and ellipsoidal-shaped aggregate particles. Aggregates are white, bulk cement paste is gray, and the interfacial transition zones are black.

because the slice does not always go through sphere centers. In this two-dimensional slice, the interfacial zone regions do not appear to percolate at all. As a further example, Fig. 11 shows slices through two other similar systems, but with both having a wider range of aggregate sizes than in Fig. 10. The right hand system in Fig. 11 is built up of ellipsoidal particle shapes.[67]

To study the percolation in 3-D of the interfacial transition zones, it is good to first consider a simple, yet nontrivial example of these ideas: a HC–SS model for monosize spherical hard spheres.[68,69] We study the percolation of the soft shell for different thicknesses of the shell ($h = a - b$) compared to the radius of the hard cores, b. The total radius of the composite particle is $a = b + h$. The relevant variable in this case is the ratio b/a, where $b/a = 0$ is just the overlapping sphere problem mentioned earlier in the chapter, and $b/a = 1$ is the random sequential absorption or random-parking problem for nonoverlapping spheres in 3-D.[70] The larger the value of b/a (i.e. the thinner the shells), the greater the value of the volume fraction of hard cores, c, that will be required and the smaller the fraction of space that will be occupied by the percolating shells. Figure 12 shows the volume fraction of the shells at percolation versus b/a. At $b/a = 0$, we get a volume fraction of shells equal to 0.29,[10] and as $b/a \to 1$, the volume fraction of the shells needed to percolate goes to zero.[71] Note that when $b/a = 0$, there are no hard cores, and we have the overlapping sphere problem. Shown also are the value of the limiting concentration $c \approx 0.38$ for monosize random parking,[70] and curves based on

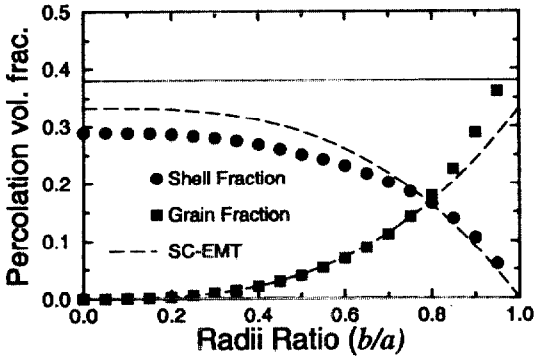

Fig. 12. Showing the volume fractions of the hard cores and the soft shells when the soft shell phase has just percolated, for monosize spherical hard core particles. The solid lines are from an effective medium theory described later in the text.

an effective medium theory.[71] Note that there is a threshold value of $b/a \approx 0.9615$ above which it does not seem possible to form connected percolating shells based on the random-parking algorithm for monosize spheres.

To study interfacial transition zone percolation in concrete, we take a fixed shell thickness to represent the interfacial transition zone, and then randomly place spherical aggregate particles that are then each surrounded by these shells. The width of the interfacial transition zone should be independent of aggregate size, as long as the median aggregate size is at least 5–10 times the median cement particle size, and will depend only on the median cement particle size.[49] The size distribution of the hard core particles are taken from measured aggregate size distributions.[64,72–74] The fraction of the total shell volume that forms part of a connected cluster is then computed as a function of the volume fraction of aggregate present.

Results for a mortar[64,73,74] are shown in Fig. 13, in which each curve shows the connectivity of the interfacial transition zones for different choices of interfacial transition zone thickness.

When comparing against portland cement mortar mercury intrusion data,[64,73,74] it was found that a choice of 20 μm for the interfacial transition zone thickness gave the best agreement with the mercury data. The mercury data gave an idea of what the percolation threshold of the interfacial transition zones was by showing a large increase in large pores intruded at the mercury breakthrough point[75] at a certain aggregate volume fraction. The width given in scanning electron microscopy studies of the interfacial transition zone,

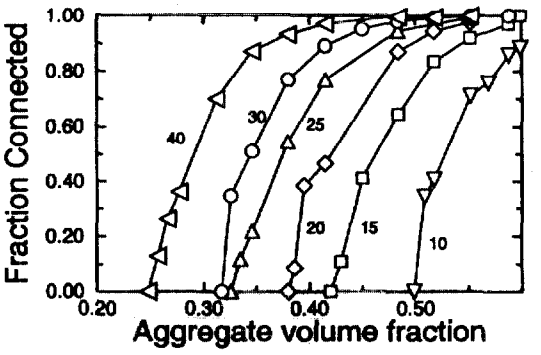

Fig. 13. Showing the fraction of the total interfacial zone volume that is a part of a percolated (continuous) cluster as a function of aggregate volume fraction and for several interfacial zone thicknesses.

30–50 μm, is defined by measuring from the aggregate edge to where the measured porosity assumes its bulk value. This would not be the width seen by mercury porosimetry, because it is probable that the larger pores will be found in the larger porosity regions nearer to the aggregate, which will be seen first by the mercury. Also, as to the effect on transport properties, the inner region of the interfacial transition zone is of more importance, since its transport properties will be higher than the outer region because of the larger pore size and porosity. The width of 20 μm given by the hard core/soft shell model is then an effective width, where this width contains the larger pores that would be important for transport. Figure 13 also shows that for an aggregate volume fraction of 40% or more and an interfacial transition zone thickness of at least 20 μm, the interfacial transition zones will be percolated at least partially, and will be fully percolated for aggregate volume fractions greater than 50%. Most concretes have aggregate volume fractions well above 50%, so that in general, we can conclude that the interfacial transition zones in usual portland cement concrete are percolated, and so will have an effect on transport properties.

The fraction of the cement paste that lies in interfacial transition zones can also be calculated using the hard core/soft shell model for a given aggregate volume fraction and particle size distribution. Results are given in Fig. 14 for a specific mortar and concrete.[64] Figure 14 shows that, for the mortar, quite a large part of the cement paste matrix lies within an interfacial transition zone, with about 20% lying within 20 μm and about 50% lying within 50 μm of an aggregate surface. For the concrete, the volume of cement paste matrix in the

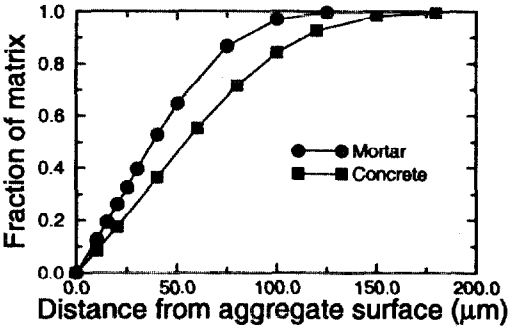

Fig. 14. Showing the fraction of the total cement paste volume fraction that lies within a given distance from an aggregate surface, for a mortar with a sand volume fraction of 0.552, and a concrete with an aggregate volume fraction of 0.646.

interfacial transition zone is smaller at each distance than for the mortar. This is related to the fact that the mortar, at an equal volume fraction of aggregate, has a much larger surface area because of the smaller size of the aggregates, and therefore, more interfacial transition zone material. This difference will also be reflected in the transport properties, as will be seen further below.

The interfacial transition zone percolation problem has also been studied for ellipsoidal aggregate particles[67] as a first look at how the aggregate shape could affect interfacial transition zone percolation. The aspect ratio of the ellipsoidal aggregates was varied between one and four, since most aggregates found in real concrete are reasonably spherical. The interfacial transition zone percolation threshold in terms of the aggregate volume fraction was found to be dependent on the aspect ratio of the aggregate. However, the interfacial transition zone percolation threshold in terms of the volume fraction of interfacial zone (paste) was not dependent on the aggregate aspect ratio.[67]

4.4. *Diffusivity/conductivity of concrete*

Concrete conducts electricity via the cement paste matrix, and the aggregates are assumed to be simply insulating obstacles to the flow of current. As was mentioned before, diffusivity is handled mathematically and physically the same way, so we specialize in conductivity language in the present discussion. Adapting the hard core/soft shell concrete model to study conductivity/diffusivity requires three input parameters: (1) the thickness of the interfacial layer, (2) the contrast in properties between this layer and the bulk

cement paste, and (3) the concentration and size distribution of the aggregates. Following the previous discussion, we will assume that all aggregates are spherical and that the interfacial transition zones are always spherical shells of constant thickness. As stated previously, while the thickness of the interfacial transition zone, h, may be as large as 50 μm, mercury intrusion measurements and modeling results[59] suggest that $h = 20$ μm is a more typical value, especially since this is the main region having higher porosity, and therefore, higher conductivity. We assume that the conductivity within the interfacial shell takes a constant value, σ_s, and that the conductivity of the cement paste, σ_p, is also constant. This is not, strictly speaking, quite true.

The actual situation is somewhat more complicated. Since the cement paste is mixed at a fixed w/c ratio, having extra porosity and thus extra water in the interfacial transition zone regions, which can occupy up to one third of the total matrix phase, means that the bulk paste must have a somewhat lower porosity and consequently a lower w/c ratio. Therefore, the conductivity of the matrix paste of a mortar or concrete cannot be simply taken as that of the cement paste from which the composite was made. Also, the interfacial transition zone region actually shows a gradient of properties, since it has a gradient in porosity.[47] Section 6 discusses this point more fully.

Since there is therefore no experimentally established value for the ratio σ_s/σ_p, we allow this parameter to vary freely in our calculations. For a given aggregate volume fraction, we have studied the dependence of the composite conductivity on the value of σ_s/σ_p. We have also studied the conductivity as a function of aggregate volume fraction for several fixed values of σ_s/σ_p. To compute the conductivity of such a model, we have adopted a random walk algorithm, used extensively in studies of disordered porous media and composite materials.[76–78]

However, it is useful to first consider the limit of dilute aggregate concentration. The composite conductivity in this regime contains important information about the conductivity and size of the interfacial transition zone. This is the case because exact analytical calculations can be made of the influence of a small volume fraction of aggregates (each of which is surrounded by an interfacial shell) placed in a matrix. For the composite to be considered to be in the dilute limit, the volume fraction of aggregates must be small enough so that particles can be treated individually and they do not affect each other. Consider monosize spherical particles of conductivity σ_1 and radius b, each surrounded by a concentric shell of thickness h and conductivity σ_2, and all

embedded in a matrix of conductivity σ_3. If the volume fraction of sand grains is denoted by c, then the composite conductivity σ, can be analytically approximated by an equation of the form $\sigma/\sigma_3 = 1 + mc + O(c^2)$, with the slope m given by[66]:

$$m = \frac{3[(\sigma_1 - \sigma_2)(2\sigma_2 + \sigma_3) + (\frac{b+h}{b})^3(\sigma_1 + 2\sigma_2)(\sigma_2 - \sigma_3)]}{[(\sigma_2 + 2\sigma_3)(\sigma_1 + 2\sigma_2) + 2(\frac{b}{b+h})^3(\sigma_1 - \sigma_2)(\sigma_2 - \sigma_3)]} m_d e f . \qquad (2)$$

To make the connection to our mortar problem, let $\sigma_1 = 0$, $h =$ the interfacial zone thickness, $\sigma_2 = \sigma_S$ (interfacial zone conductivity), and $\sigma_3 = \sigma_p$ (bulk cement paste conductivity). For the random mortar model, or indeed for a real mortar, there is a size distribution of sand grain radii b_i, while the value of h is fixed. This implies that the slope m_i for each kind of particle will be a function of b_i, because the parameter $[(b_i + h)/b_i]^3$ will be different for each particle. In a system with N different sand particle sizes, each with volume fraction c_i, the average slope $\langle m \rangle$ is then defined by

$$\langle m \rangle = \sum_{i=1}^{N} \frac{m_i c_i}{c} , \qquad (3)$$

where

$$\sum_{i=1}^{N} c_i = c . \qquad (4)$$

This dilute limit problem can also be solved in the case where a gradient of properties exists around the aggregate.[79]

Using the four-diameter sand particle model distribution for a mortar mentioned previously,[66] we can find the value of $\langle m \rangle$ averaged over the appropriately weighted four values of b_i.[66] Figure 15 shows a graph of this average slope $\langle m \rangle$ as a function of σ_s/σ_p.

Note in the limit of $\sigma_s/\sigma_p = 1$, the slope $\langle m \rangle = -3/2$, which is the known exact result for insulating spherical inclusions of any size distribution.[80] The marked point on the graph is at $\sigma_s/\sigma_p \approx 8.26$, which is the point at which the slope $\langle m \rangle = 0$. At this value, to linear order in c, adding a few sand grains would have no effect on the overall conductivity. Here one has a perfect balance between the negative influence of the insulating sand grains and the positive effect of the enhanced conductivity in the interfacial shells.

The only exact results available for general three-dimensional composite materials, in addition to the dilute limits presented above, are variational

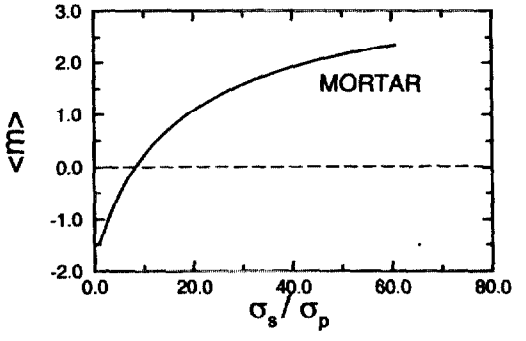

Fig. 15. The exact initial slope of the conductivity, in the limit of dilute sand concentration, is shown as a function of σ_s/σ_p for the four size model mortar.

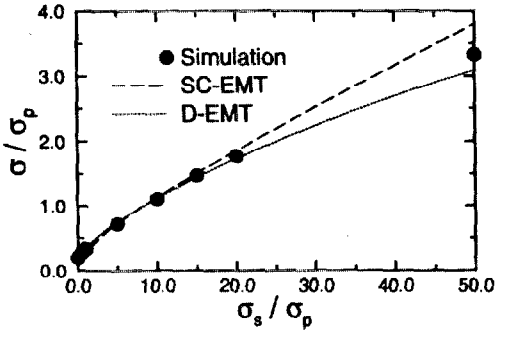

Fig. 16. Composite conductivity for the four size model mortar is plotted versus the interfacial zone conductivity. [Both are normalized by bulk paste conductivity.] The solid dots are the random walk data; also shown are the effective medium results (SC = self consistent and D = differential).

bounds.[81] However, effective medium theory (EMT) can often be employed to estimate composite properties at arbitrary volume fractions of the phases.[82,83] By EMT, we mean only those theories that properly describe the dilute limit, and are then built up via some sort of averaging assumption into approximate analytical equations. The two examples that have been previously considered are the self-consistent[82] and the differential[83] methods.

In Fig. 16, we present the random walk simulation results for the same four-diameter aggregate mortar model together with the predictions of the differential (D-EMT) and self-consistent (SC-EMT) effective medium theories.[71]

The simulations were of how the effective conductivity, at a single aggregate volume fraction, 55%, and a single interfacial transition zone thickness, 20 μm, varied as a function of the conductivity of the interfacial transition zone phase σ_s, expressed as the dimensionless ratio σ_s/σ_p. The overall shape of the curves is concave down. In this case, the effective conductivity could at most be linear in σ_s/σ_p, for the following reason. If the two conducting phases, interfacial transition zone and bulk cement paste, were exactly in parallel geometrically, then the overall conductivity would be given by a simple linear combination of the two phase conductivities, and as σ_s increased, the overall conductivity would increase linearly. Since the microstructure is such that these two cement paste phases are not in parallel, the curve must be sublinear, or concave down. As $\sigma_s/\sigma_p \to \infty$, the curve will eventually become straight as predicted,[66] since the interfacial transition zone conductivity will dominate the effective conductivity. Note that by the point $\sigma_s/\sigma_p = 20$, the effective conductivity is almost double the pure matrix conductivity, $\sigma/\sigma_p \approx 1.8$.

The data in Fig. 16 indicate that to achieve an overall conductivity that is equal to the bulk cement paste conductivity, the value of σ_s/σ_p must be equal to approximately 8. This is remarkably close to the dilute limit result $\sigma_s/\sigma_p \approx 8.26$ found in Fig. 15. Because the dilute limit seems to define an essential feature of the overall curve, effective medium theories that are based on the dilute limit have a good possibility of successfully predicting the essential structure of the composite conductivity. The two EMT's displayed in Fig. 16 do show reasonably good agreement with the simulation data.

Figure 17 shows computed conductivity data for the random mortar model as a function of sand volume fraction, for $\sigma_s/\sigma_p = 20$, 5, and 1.

The curve for $\sigma_s/\sigma_p = 20$ is concave up, with an initial slope that is positive, since $\sigma_s/\sigma_p = 20 > 8.26$. Both EMT's predict that when the inital slope is positive, the value of the effective conductivity σ_s/σ_p, will always be greater than 1. The simulation data do obey this prediction. The value of $\sigma_s/\sigma_p = 20$ is not high enough to see clear evidence of the interfacial zone percolation threshold, which for much higher values of σ_s/σ_p, would manifest itself as a sharply increasing conductivity near the percolation threshold. The $\sigma_s/\sigma_p = 5$ and 1 curves have negative initial slopes, and the effective conductivities remain below one, as predicted also by EMT. The $\sigma_s/\sigma_p = 1$ curve roughly follows a 3/2 power law in the total cement paste volume fraction, as would be expected since there is no difference between interfacial zone and bulk cement paste in this case.[80]

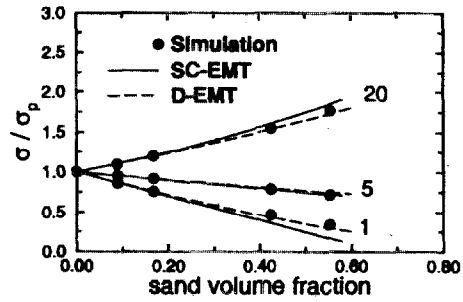

Fig. 17. Composite conductivities (calculated by random walk simulations) for the random model are shown as a function of sand concentration for three values of the interfacial zone conductivity. Also shown are the predictions of the SC- and D-EMT calculations, with the same normalization as in the previous figure.

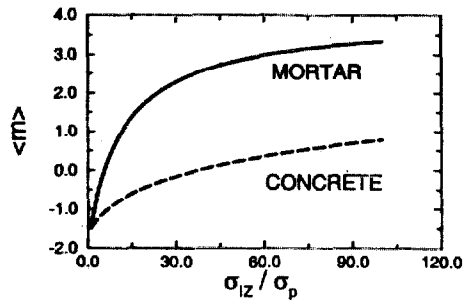

Fig. 18. The exact initial slope of the conductivity, in the limit of dilute sand concentration, is shown as a function of σ_s/σ_p for a typical mortar and a typical concrete aggregate particle size distribution.

Figure 18 shows analytical results for $\langle m \rangle$ for a typical mortar[84] and a typical concrete.[72] At a given value of σ_s/σ_p, the value of $\langle m \rangle$ for the mortar is always higher than that for the concrete. This comes back to the same point made earlier, that the mortar has a larger surface area at a given volume fraction, due to the smaller average particle size, and so the interfacial zone has a larger volume and plays a bigger role in its composite properties than it does in the concrete's composite properties.

5. C–S–H

The C–S–H phase plays the role as the glue that holds cement paste together. We now go down from the micrometer length scale of cement paste and the

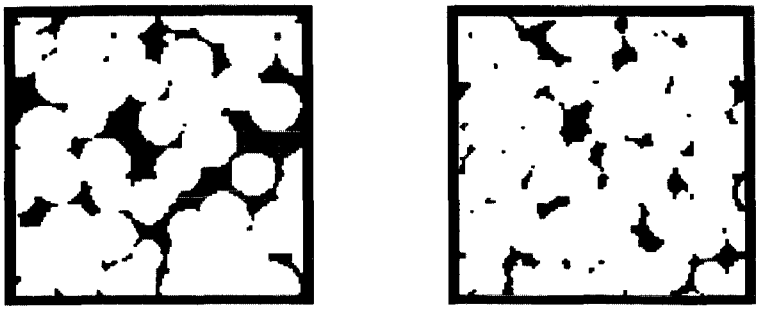

Fig. 19. Two-dimensional slices from three-dimensional model microstructures of the C–S–H gel at the scale of nanometers. Right: micro model (25 × 25 nm), left: macro model (250 × 250 nm). White = solid, black = pore.

millimeter scale of concrete, to examine models for the nanostructure of the nanometer-scaled C–S–H phase. Little is known of the actual details of the atomic structure of C–S–H, as it is amorphous, so the model focuses on the nanometer scale.

At the scale of nanometers, the C–S–H gel is modeled as a two-level structure of partialy overlapping spherical particles.[85] At the macro-level, the 2-D cross-section of the larger 40 nm spherical agglomerates shown in the right-hand image of Fig. 19 are each composed of smaller 5 nm diameter micro level particles, as shown in the left-hand image of Fig. 19.

The particle sizes and the total porosity at each level have been chosen to be consistent with experimental data from small angle neutron scattering[7] and sorption measurements.[86] The models are generated in continuum space (in a three-dimensional cube with periodic boundaries) and subsequently digitized into a 3-D digital image for the evaluation of properties. The structural models have been validated by computing sorption isotherms and the pore volume accessible to molecules of varying diameters, and comparing to experimental results.[85] Computational techniques have also been applied to computing both the conductivity/diffusivity and the permeability[22] of the macro-level gel structure, with reasonable agreement with experiment.

6. Multiscale Models for the Ionic Diffusivity

As has been mentioned earlier, computer modeling of the properties and performance of cement-based materials is complicated by the large range of relevant size scales. Processes occurring in the nanometer-sized pores ultimately affect

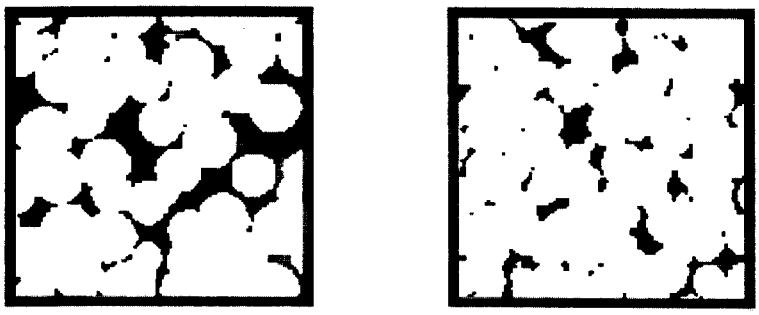

Fig. 19. Two-dimensional slices from three-dimensional model microstructures of the C–S–H gel at the scale of nanometers. Right: micro model (25 × 25 nm), left: macro model (250 × 250 nm). White = solid, black = pore.

millimeter scale of concrete, to examine models for the nanostructure of the nanometer-scaled C–S–H phase. Little is known of the actual details of the atomic structure of C–S–H, as it is amorphous, so the model focuses on the nanometer scale.

At the scale of nanometers, the C–S–H gel is modeled as a two-level structure of partialy overlapping spherical particles.[85] At the macro-level, the 2-D cross-section of the larger 40 nm spherical agglomerates shown in the right-hand image of Fig. 19 are each composed of smaller 5 nm diameter micro level particles, as shown in the left-hand image of Fig. 19.

The particle sizes and the total porosity at each level have been chosen to be consistent with experimental data from small angle neutron scattering[7] and sorption measurements.[86] The models are generated in continuum space (in a three-dimensional cube with periodic boundaries) and subsequently digitized into a 3-D digital image for the evaluation of properties. The structural models have been validated by computing sorption isotherms and the pore volume accessible to molecules of varying diameters, and comparing to experimental results.[85] Computational techniques have also been applied to computing both the conductivity/diffusivity and the permeability[22] of the macro-level gel structure, with reasonable agreement with experiment.

6. Multiscale Models for the Ionic Diffusivity

As has been mentioned earlier, computer modeling of the properties and performance of cement-based materials is complicated by the large range of relevant size scales. Processes occurring in the nanometer-sized pores ultimately affect

the performance of these materials at larger length scales. At present, it is impossible to simultaneously handle all these length scales, from nanometers to millimeters and larger, using a single computer-based model. One approach to alleviating this complication is the development of a suite of models, consisting of individual digital-image-based or continuum structural models for the calcium silicate hydrate gel at the nanometer level, the hydrated cement paste at the micrometer level, and a mortar or concrete at the millimeter level. Computations performed at one level provide input properties to be used in simulations of performance at the next higher level. This is the ultimate goal of this research, and will be demonstrated for the property of ionic diffusivity in saturated concrete, using the models discussed in previous sections. Here the relative diffusivity of concrete is computed. The relative diffusivity is defined as the ratio of the diffusivity of ions in a composite medium to their diffusivity in bulk water. Based on the Nernst–Einstein relation, the relative diffusivity D/D_o is equivalent to the relative conductivity $\Gamma = \sigma/\sigma_o$. In this case, saturated means that all the pore space is filled with the same pore fluid.

The Nernst–Einstein equation is used to determine the diffusivity by solving the equivalent electrical problem for the electrical conductivity of the composite material.[32] As was discussed above, to solve for the properties of these models, the properties of each phase in a microstructure must be known or assumed. The multiscale approach we use is to utilize properties computed at one scale level of modeling as input into the computation procedures employed at a higher scale. For example, the conductivity/diffusivity computed for the C–S–H gel nanostructure model can be used as an input property into the cement paste microstructure model, so that the conductivity/diffusivity of cement paste can be computed as a function of w/c and α. Likewise, the diffusivity computed for bulk and interfacial transition zone cement paste can be used in the model of concrete at the level of millimeters, to compute the diffusivity of a concrete; the quantity of actual interest to a design or structural engineer.

The first step is the computation of the relative diffusivity of the C–S–H gel. Using the electrical analogy and the nanostructural model shown in the top portion of Fig. 19, a value of 1/300 is computed for the relative diffusivity of the gel. Here, we assume that diffusive transport occurs only in the cluster-level pores and not in the much smaller pores shown in the particle-level model in the top portion of Fig. 19. This is a reasonable assumption, since these smaller, nanometer-sized pores are of the order of the size of a water molecule and would be virtually inaccessible to many diffusing ions. A further assumption

is that this relative diffusivity value is characteristic of all C–S–H gel regardless of cement composition or when during the hydration process the C–S–H is produced. When trying to match simulation results for the ionic diffusivity of cement paste to experimental results by adjusting the value of the relative diffusivity assigned to the C–S–H phase, we found a value of approximately 1/400,[32] so reasonably good agreement, albeit in an indirect way, has been obtained for the nanometer-scale model.

The second step is to use the value computed for the relative diffusivity of the C–S–H gel in a computation of the relative diffusivity of cement pastes of various w/c ratios and degrees of hydration. A diffusivity value of 1 is assigned to the capillary porosity, while the unhydrated cement and calcium hydroxide are assigned diffusivities of 0 since they contain no porosity. Again using the electrical analogy, computations performed for a variety of 100^3 element microstructures have resulted in the development of an equation which relates relative diffusivity to the capillary porosity of the cement paste. Good agreement has been observed in comparing these computed model values to ones measured experimentally both for chloride ion diffusivity[31,36] and cement paste conductivity.[30]

Finally, the relative diffusivity values computed for cement paste can be used as input into the structural model for mortar to determine the effect of aggregates and their surrounding interfacial zones on the diffusivity of the mortar, D_M. At this level, one must select the thickness of the interfacial zone paste and the value of its diffusivity D_{ITZ} compared to that of the bulk paste D_P. Techniques like those described in Refs. 66 and 71 can then be used to compute D_M. Care must be taken to properly allow for the redistribution of cement between the interfacial transition zone regions and the bulk cement paste. For a given w/c cement paste surrounding the aggregate grains, higher porosity in the interfacial transition zone region means a lower porosity in the bulk cement paste regions. This redistribution of cement determines the correct ratio of diffusivities that is needed to be used in the models of Refs. 66 and 71. A technique that approximately allows for this redistribution has been described.[79,88,89]

7. Summary

It has been shown that theoretical understanding of the microstructure–transport property relationships of concrete, from the cement paste up to the full composite, can be based on the ideas of pore size and connectivity, with

connectivity defined rigorously using percolation concepts. These concepts give a fairly complete, although at present mainly qualitative, picture of how transport properties depend on microstructure in concrete. Percolation phenomena in concrete include the setting of cement paste, the connectivity of the C–S–H gel phase, the disconnection of the capillary pore space in cement paste, the effect of leaching of calcium hydroxide on the transport properties of cement paste, and the connection of the interfacial transition zones in concrete. Like the material itself, percolation phenomena are important over many length scales, and since more than one phase of the concrete composite is simultaneously percolated, concrete must be considered to be an interpenetrating phase composite.[86]

The use of a set of multiscale microstructure models to investigate transport and mechanical properties of concrete has been demonstrated. By relating microstructure to properties at all relevant size scales, a more complete understanding of the influence of microstructure and the underlying physical processes on the performance of these composite materials can be obtained. For the case of chloride diffusivity, a nearly complete set of results has been presented.[88,89] As the structural modeling and computational capabilities described herein continue to evolve, their use as a tool in the design of a concrete with desired properties and service life should become a reality. The reader should note that an electronic version of this paper, many of the references of this paper, plus many color images, are available in *An Electronic Monograph: Modelling the Structure and Properties of Cement-Based Materials* at http://ciks.cbt.nist.gov/garboczi/.

Acknowledgments

The authors thank the High Performance Construction Materials and Systems program at NIST and the National Science Foundation Science and Technology Center for Advanced Cement-Based Materials for partial funding of this work. We also thank our many collaborators in this research, whose names are listed throughout the references.

Appendix: Computational Details

The various simulations described in this paper have been run using many different computers, over a period of ten years, for many different system sizes. The run times and memory requirements of the main simulations described

in the text are given below for modern computers that are in general use at present (1998).

The hydration code is in C. A typical system size is 100^3 for a $w/c = 0.4$ cement paste. In this case, the initial solids volume fraction is about 44%. Using a 333 MHz Pentium II processor, with 128 MB of memory, running RedHat 5.1 Linux, and using the C compiler that comes with the operating system, this system takes 3.6 MB of memory, 7 s per hydration cycle when the pore space percolation is checked every cycle, and 4.8 s per hydration cycle with no percolation check.

Computing the conductivity of this same system, but now in Fortran 77 on a Cray 90, one processor requires about 5 min of CPU time, and about 80 MB of memory. This is using a conjugate gradient relaxation process with a finite difference routine (for details of the code, see http://ciks.cbt.nist.gov/garboczi/, Chapter 2).

The code for performing the concrete hard core/soft shell model is in C. To generate a 529 000 particle system, and perform a percolation check for one value of the shell thickness, 845 s and 87 MB of memory are required on the same Linux machine mentioned above. When 10 000 random walkers were used to compute the conductivity of the same system, about 428 additional CPU seconds were required to take 1000 steps per walker, with very little extra memory required.

References

1. F. M. Lea, *The Chemistry of Cement and Concrete* (St. Martin's Press, New York, 1956), Chapter 1.
2. J. F. Young, "A review of the pore structure of cement paste and concrete and its influence on permeability," in *Permeability of Concrete*, ed. D. Whiting and A. Walitt, ACI SP-108 (American Concrete Institute, Detroit, 1988).
3. E. J. Garboczi, *Materials and Structures* **26**, 191 (1993).
4. H. F. W. Taylor, *Cement Chemistry* (Academic Press, San Diego, 1990).
5. R. Maggion, PhD thesis (L'Universit D'Orleans, France 1992).
6. D. Viehland, J. F. Li, L. J. Yuan, and Z. Xu, *J. Amer. Ceram. Soc.* **79**, 1731 (1996).
7. A. J. Allen, R. C. Oberthur, D. Pearsons, P. Schofield, and C. R. Wilding, *Phil. Mag.* **B56**(3), 263 (1987).
8. M. Sahimi, in *Annual Reviews of Computational Physics II*, ed. D. Stauffer (World Scientific, Singapore, 1995), p. 175.
9. E. J. Garboczi, M. F. Thorpe, M. DeVries, and A. R. Day, *Phys. Rev.* **A43**, 6473 (1991).

10. E. J. Garboczi, K. A. Snyder, J. F. Douglas, and M. F. Thorpe, *Phys. Rev.* **E52**, 819 (1995).
11. J. Kertesz, *J. Phys. Lett.* **42**, L393 (1981); W. T. Elam, A. R. Kerstein, and J. J. Rehr, *Phys. Rev. Lett.* **52**, 1516 (1984); S. B. Lee and S. Torquato, *J. Chem. Phys.* **89**, 3258 (1988).
12. D. P. Bentz and P. E. Stutzman, "SEM analysis and computer modeling of hydration of portland cement particles," in *ASTM STP 1215*, ed. S. M. DeHayes and D. Stark (American Society for Testing and Materials, Philadelphia, 1994), p. 60.
13. *High-Performance Construction Materials and Systems: An Essential Program for America and Its Infrastructure*, Technical Report 93-5011 (Civil Engineering Research Foundation, Washington, D.C., 1993).
14. D. P. Bentz, P. C. Coveney, E. J. Garboczi, M. F. Kleyn, and P. E. Stutzman, *Modeling and Simulation in Materials Science and Engineering* **2**, 783 (1994).
15. D. P. Bentz and E. J. Garboczi, *Guide to Using HYDRA3D: A Three-Dimensional Digital-Image-Based Cement Microstructure Model*, NISTIR 4746 (U.S. Department of Commerce, 1992).
16. W.-G. Lei, "Rheological studies and percolation modeling of microstructure development of fresh cement paste," PhD Thesis (University of Illinois, Department of Materials Science and Engineering, 1995).
17. Y. Chen and I. Odler, *Cem. Conc. Res.* **22**, 1130 (1992).
18. ASTM C-191 (1992), Standard Test Method for Time of Setting of Hydraulic Cement by Vicat Needle, American Society for Testing of Materials, Philadelphia, Pa.
19. C. M. Sayers and R. L. Grenfell, *Ultrasonics* **31**, 147 (1993).
20. S. P. Jiang, J. C. Mutin, and A. Nonat, in *Proceedings of the 9th International Congress on the Chemistry of Cement, Vol. III*, p. 17, New Delhi, India.
21. D. P. Bentz and E. J. Garboczi, *Cem. Conc. Res.* **21**, 325 (1991).
22. D. P. Bentz, E. J. Garboczi, and N. S. Martys, "Application of digital-image-based models to microstructure, transport properties, and degradation of cement-based materials," in *The Modeling of Microstructure and Its Potential for Studying Transport Properties and Durability*, eds. H. Jennings, J. Kropp, and K. Scrivener, p. 167.
23. R. T. Coverdale, "Microstructural analysis of cement paste using a computer model of impedance spectroscopy," PhD thesis (Northwestern University, Department of Materials Science and Engineering, 1993).
24. C. Legrand and E. Wirquin, "Effects of the initial structure of the cement paste in fresh concrete on the first developments of strength. Influence of superplasticizers," in *Proc. 9th International Congress on the Chemistry of Cement, Vol. V*, 95–99 (New Delhi, India, 1992).
25. S. P. Jiang, J. C. Mutin, and A. Nonat, in *Proc. 3rd Beijing International Symposium on Cement and Concrete*, 126–131 (China Building Materials Academy, 1993).

26. W. G. Lei, L. J. Struble, D. P. Bentz, E. Schlangen, and E. J. Garboczi, in preparation.
27. T. C. Powers, L. E. Copeland, and H. M. Mann, *PCA Bulletin* **10** (1959).
28. D. P. Bentz, unpublished.
29. B. J. Christensen, T. O. Mason, and H. M. Jennings, *J. Amer. Ceram. Soc.* **75**, 935 (1992).
30. R. A. Olson, B. J. Christensen, R. T. Coverdale, S. J. Ford, G. M. Moss, H. M. Jennings, T. O. Mason, and E. J. Garboczi, *J. Mater. Sci.* **30**, 5078 (1995).
31. P. Halamickova, R. J. Detwiler, D. P. Bentz, and E. J. Garboczi, *Cem. Conc. Res.* **25**, 790 (1995).
32. E. J. Garboczi and D. P. Bentz, *J. Mater. Sci.* **27**, 2083 (1992).
33. A. Atkinson and A. K. Nickerson, *J. Mater. Sci.* **19**, 3068 (1984).
34. R. T. Coverdale, B. J. Christensen, H. M. Jennings, T. O. Mason, D. P. Bentz, and E. J. Garboczi, *J. Mater. Sci.* **30**, 712 (1995).
35. R. T. Coverdale, B. J. Christensen, T. O. Mason, H. M. Jennings, and E. J. Garboczi, *J. Mater. Sci.* **29**, 4984 (1994).
36. B. J. Christensen, T. O. Mason, H. M. Jennings, D. P. Bentz, and E. J. Garboczi, in *Advanced Cementitious Systems: Mechanisms and Properties* **245**, 259 (Materials Research Society, Pittsburgh, 1992).
37. B. J. Christensen, "Microstructure studies of hydrating portland cement-based materials using impedance spectroscopy," PhD thesis (Northwestern University, Department of Materials Science and Engineering, 1993).
38. B. J. Christensen, T. O. Mason, R. T. Coverdale, H. M. Jennings, R. A. Olson, and E. J. Garboczi, *J. Am. Ceram. Soc.* **77**, 2789 (1994).
39. D. P. Bentz and E. J. Garboczi, *Materials and Structures* **25**, 523 (1992).
40. E. Revertegat, C. Richet, and P. Gegout, *Cem. Conc. Res.* **22**, 259 (1992).
41. P. K. Mehta and P. J. M. Monteiro, *Concrete: Structure, Properties, and Materials* (Prentice-Hall, Englewood Cliffs, New Jersey, 1993).
42. D. P. Bentz, E. Schlangen, and E. J. Garboczi, "Computer simulation of interfacial zone microstructure and its effect on the properties of cement-based composites," in *Materials Science of Concrete IV*, eds. J. P. Skalny and S. Mindess (American Ceramic Society, Westerville, 1994), p. 155.
43. S. Diamond, S. Mindess, and J. Lovell, in *Liasons Pater de Ciment Materiaux Associes* (RILEM, Toulose, France, 1982), p. C42.
44. D. P. Bentz, N. S. Martys, P. E. Stutzman, M. S. Levenson, E. J. Garboczi, J. Dunsmuir, and L. M. Schwartz, in *Microstructure of Cement-Based Systems/Bonding and Interfaces in Cementitious Materials* (Materials Research Society, Pittsburgh, 1995), p. 77.
45. J. Farran, *Rev. Mater. Const.* **490–491**, 155 (1956).
46. J. C. Maso, "The bond between aggregates and hydrated cement paste," in *Proc. 7th International Congress on the Chemistry of Cement* I, VII-1/3 (Paris, 1980).
47. K. Scrivener, "The Microstructure of Concrete," in *Materials Science of Concrete I*, ed. J. Skalny (American Ceramic Society, Westerville, 1990).

48. E. J. Garboczi and D. P. Bentz, *J. Mater. Res.* **6**, 196 (1991).
49. D. P. Bentz, E. J. Garboczi, and P. E. Stutzman, "Computer modelling of the interfacial zone in concrete," in *Interfaces in Cementitious Composites*, ed. J. Maso (E and FN Spon, London, 1992), p. 107.
50. D. P. Bentz and E. J. Garboczi, *Am. Conc. Inst. Mater. J.* **88**, 518 (1991).
51. Z. Hashin, *J. App. Mech.* **50**, 481 (1983).
52. L. O. Nilsson and J. P. Ollivier, eds., "Steady-state diffusion characteristics of cementitious materials," in *Chloride Penetration into Concrete* (1997).
53. A. Delagrave, J. P. Bigas, J. P. Ollivier, J. Marchand, and M. Pigeon, *Adv. Cem.-Based Mater.* **5**, 86 (1997).
54. Y. F. Houst, H. Sadouki, and F. H. Wittmann, in *Interfaces in Cementitious Composites*, ed. J. Maso (E and FN Spon, London, 1992), p. 279.
55. R. W. Zimmerman, M. S. King, and P. J. M. Monteiro, *Cem. Con. Res.* **16**, 239 (1986).
56. A. U. Nilsen and P. J. M. Monteiro, *Cem. Conc. Res.* **23**, 147 (1993).
57. M. D. Cohen, A. Goldman, and W. F. Chen, *Cem. Conc. Res.* **24**, 95 (1994).
58. K. A. Snyder and J. R. Clifton, "Measures of air-void spacing," in *Proc. International Conference on Building Materials*, p. 155 (Weimar, Germany, 1994).
59. K. A. Snyder, J. R. Clifton, and L. I. Knab, in *Proc. International Conference on Building Materials*, p. 139 (Weimar, Germany, 1994).
60. A. I. Rashed and R. B. Williamson, *J. Mater. Res.* **6**, 2004 (1991).
61. E. W. Washburn, *Proc. Natl. Acad. Sci. USA* **7**, 115 (1921).
62. J. van Brakel (ed.), *A Special Issue Devoted to Mercury Porosimetry*, Powder Tech. **29**, 1 (1981).
63. E. J. Garboczi and D. P. Bentz, *Ceramic Transactions* **16**, 365 (1991).
64. D. N. Winslow, M. Cohen, D. P. Bentz, K. A. Snyder, and E. J. Garboczi, *Cem. Conc. Res.* **24**, 25 (1994).
65. S. Torquato, *J. Chem. Phys.* **85**, 6248 (1986).
66. E. J. Garboczi, D. P. Bentz, and L. M. Schwartz, *Adv. Cem.-Based Mater.* **2**, 169 (1995).
67. D. P. Bentz, J. T. G. Hwang, C. Hagwood, E. J. Garboczi, K. A. Snyder, N. Buenfeld, and K. L. Scrivener, "Interfacial zone percolation in concrete: Effects of interfacial thickness and aggregate shape," in *Microstructure of Cement-Based Systems/Bonding and Interfaces in Cementitious Materials*, ed. S. Diamond *et al.* (Materials Research Society, Pittsburgh, 1995), p. 437.
68. G. E. Pike and C. H. Seager, *Phys. Rev.* **B10**, 1421 (1974).
69. A. L. Bug, S. A. Safran, G. S. Grest, and I. Webman, *Phys. Rev. Lett.* **55**, 1896 (1985).
70. D. W. Cooper, *Phys. Rev.* **A38**, 522 (1988).
71. L. M. Schwartz, E. J. Garboczi, and D. P. Bentz, *J. App. Phys.* **78**, 58988 (1995).
72. D. Winslow and D. Liu, *Cem. Conc. Res.* **20**, 227 (1990).
73. K. A. Snyder, D. N. Winslow, D. P. Bentz, and E. J. Garboczi, "Effects of interfacial transition zone percolation on cement-based composite transport

properties," in *Advanced Cementitious Systems: Mechanisms and Properties*, eds. F. P. Glasser, G. J. McCarthy, J. F. Young, T. O. Mason, and P. L. Pratt (Materials Research Society, Pittsburgh, 1992), p. 265.
74. K. A. Snyder, D. N. Winslow, D. P. Bentz, and E. J. Garboczi, "Interfacial zone percolation in cement-aggregate composites," in *Interfaces in Cementitious Composites*, ed. J. Maso (E and FN Spon, London, 1992), p. 259.
75. D. N. Winslow and S. Diamond, *ASTM J. Mater.* **5**, 564 (1970).
76. L. M. Schwartz and J. R. Banavar, *Phys. Rev.* **B39**, 11965 (1989).
77. I. C. Kim and S. Torquato, *Phys. Rev.* **A43**, 3198 (1991).
78. D. C. Hong, H. E. Stanley, A. Conoglio, and A. Bunde, *Phys. Rev.* **B33**, 4564 (1986).
79. E. J. Garboczi and D. P. Bentz, *Adv. Cem.-Based Mater.* **6**, 99 (1997).
80. R. E. De La Rue and C. W. Tobias, *J. Electrochemical Soc.* **106**, 827 (1959).
81. S. Torquato, *Appl. Mech. Rev.* **44**, 37 (1991).
82. Z. Hashin, *J. Composite Mater.* **2**, 284 (1968).
83. McLaughlin, *Int. J. Eng. Sci.* **15**, 237 (1977).
84. "ASTM Standard C-109," in *ASTM Annual Book of Standards 04.01: Cement; Lime; Gypsum* (ASTM, Philadelphia, 1995).
85. D. P. Bentz, D. A. Quenard, V. Baroghel-Bouny, E. J. Garboczi, and H. M. Jennings, *Materials and Structures* **28**, 450 (1995).
86. V. Baroghel-Bouny, PhD thesis (L'ecole Nationale des Ponts et Chaussees, France, 1994).
87. D. R. Clarke, *J. Am. Ceram. Soc.* **75**, 739 (1992).
88. D. P. Bentz, E. J. Garboczi, and E. S. Lagergren, *ASTM Cement and Aggregates* **20**, 129 (1998).
89. E. J. Garboczi and D. P. Bentz, *Adv. Cem.-Based Mater.* **8**, 77 (1998).